

Flexible and Printed Electronics



PAPER

Understanding and mitigating process drift in aerosol jet printing

RECEIVED
11 November 2019

REVISED
18 December 2019

ACCEPTED FOR PUBLICATION
22 January 2020

PUBLISHED
12 February 2020

Rebecca R Tafoya and Ethan B Secor

Sandia National Laboratories, Albuquerque, NM 87185, United States of America

E-mail: ebsecor@sandia.gov

Keywords: flexible electronics, printed electronics, additive manufacturing, aerosol jet printing

Supplementary material for this article is available [online](#)

Abstract

Aerosol jet printing offers a versatile, high-resolution prototyping capability for flexible and hybrid electronics. Despite its rapid growth in recent years, persistent problems such as process drift hinder the adoption of this technology in production environments. Here we explore underlying causes of process drift during aerosol jet printing and introduce an engineered solution to improve deposition stability. It is shown that the ink level within the cartridge is a critical factor in determining atomization efficiency, such that the reduction in ink volume resulting from printing itself can induce significant and systematic process drift. By integrating a custom 3D-printed cartridge with an ink recirculation system, ink composition and level within the cartridge are better maintained. This strategy allows extended duration printing with improved stability, as evidenced by 30 h of printing over 5 production runs. This provides an important tool for extending the duration and improving reliability for aerosol jet printing, a key factor for integration in practical manufacturing operations.

Introduction

Printed, flexible, and hybrid electronics offer a compelling platform for emerging applications spanning consumer devices, wireless connectivity, and distributed sensing [1–3]. Among the relevant manufacturing technologies for these systems, digital techniques are well-suited to rapid prototyping and smart fabrication. Aerosol jet printing, in particular, offers a promising combination of digital control, non-contact deposition, fine patterning resolution, and broad materials compatibility [4–6]. Based on these attributes, this method has attracted interest for hybrid electronics manufacturing [7–10], logic circuits [11–13], energy devices [14–16], and sensors [17–20]. Despite its potential, more widespread adoption of aerosol jet printing is hindered by process drift. While seldom discussed in research papers, the aerosol deposition rate can vary significantly, even over relatively short print durations [21]. This is a notable barrier to industrial applications, leads to significant material waste, and confounds process optimization efforts [22]. While strategies have been introduced to monitor and respond to process drift, these do not address underlying causes [22–24]. Recent efforts have explored the physics of the technology to better

understand print outputs such as line resolution and overspray [25–28], but a basic understanding of print stability remains lacking. Here we explore the underlying causes of process drift during aerosol jet printing and introduce a strategy to mitigate this problem at its source.

During aerosol jet printing, a liquid ink containing functional materials is atomized to produce 1–5 μm droplets. These droplets are picked up by a carrier gas stream and transported to the printhead, where an annular sheath gas flow surrounds the aerosol stream. This collimates the aerosol flow and accelerates it through a narrow deposition nozzle, typically 100–300 μm in diameter. Under typical conditions, this results in a 10–100 m s^{-1} jet originating 1–5 mm above a substrate. The high inertia of the aerosol droplets causes them to deviate from the gas flow stream and impact the substrate, resulting in high resolution (20–100 μm) features. Process drift can arise from several sources, including variation in atomization yield and ink composition, both of which affect drying kinetics within the printhead and can lead to unexpected outcomes [27]. Depending on the ink and process parameters, this drift can be significant. For example, Smith, *et al* observed a doubling in the cross-sectional area of silver lines after only ~ 20 min

printing, while the majority of published reports neglect to report print stability results entirely [21]. While process drift is present, efforts to optimize the process face significant challenges. In some cases, this leads researchers to discard ink and refill the cartridge periodically, leading to severe material waste. This is also a clear barrier to more widespread industrial adoption of this method, in that print stability and reliability are prerequisites and in many cases more critical than peak performance metrics such as resolution.

Here we explore the basic mechanisms for process drift, related to variation in the ink composition and loading level, using a combination of theory and experiments. Based on the results, we introduce a recirculating cartridge that improves stability and allows for extended duration printing. While this does not provide a complete solution for process control, it provides an important tool by addressing the underlying causes of drift. Using this custom cartridge, printing over a period of 30 h during 5 separate production runs is demonstrated, supporting this promising strategy to improve the application scope and industrial relevance of aerosol jet printing.

Experimental methods

Materials

Printing experiments used a magnetite nanoparticle ink based on commercially available nanoparticles from UT Dots, Inc. The base material, UTDMI-SD, is a viscous paste containing magnetite nanoparticles in xylenes. A stock solution is prepared from this by diluting the paste with xylenes in a 1:4 UTDMI:xylenes ratio (w/w). The ink for aerosol jet printing is prepared by combining this stock solution, xylenes, and terpineol in a 5:31:4 (v/v) mixture. This ink is mixed using a laboratory shaker to yield a low viscosity, brown dispersion.

Aerosol jet printing

All printing experiments were performed on a custom-built aerosol jet printer based on a modified IDS Nanojet system. Custom-designed printer cartridges were employed, along with a custom printhead using a 250 μm diameter nozzle orifice. For typical experiments, a series of 2×2 mm films was printed, each one designed to take 3 min. After each film, the flow rates are changed. After each set of 10 films, a line is printed to track line width during the process. Typical printing conditions were 36 V atomizer setting (~ 20 W), 8–14 sccm aerosol carrier gas flow rate, a sheath flow rate of $3 \times$ the aerosol flow rate, 17 $^{\circ}\text{C}$ cartridge temperature, 60 $^{\circ}\text{C}$ substrate temperature, and a print speed of 2.5 mm s $^{-1}$. For stability experiments without the recirculating cartridge, an initial volume of 2 ml ink was used. Following printing, all

samples were heated to 150 $^{\circ}\text{C}$ for 45 min to ensure complete drying.

Characterization

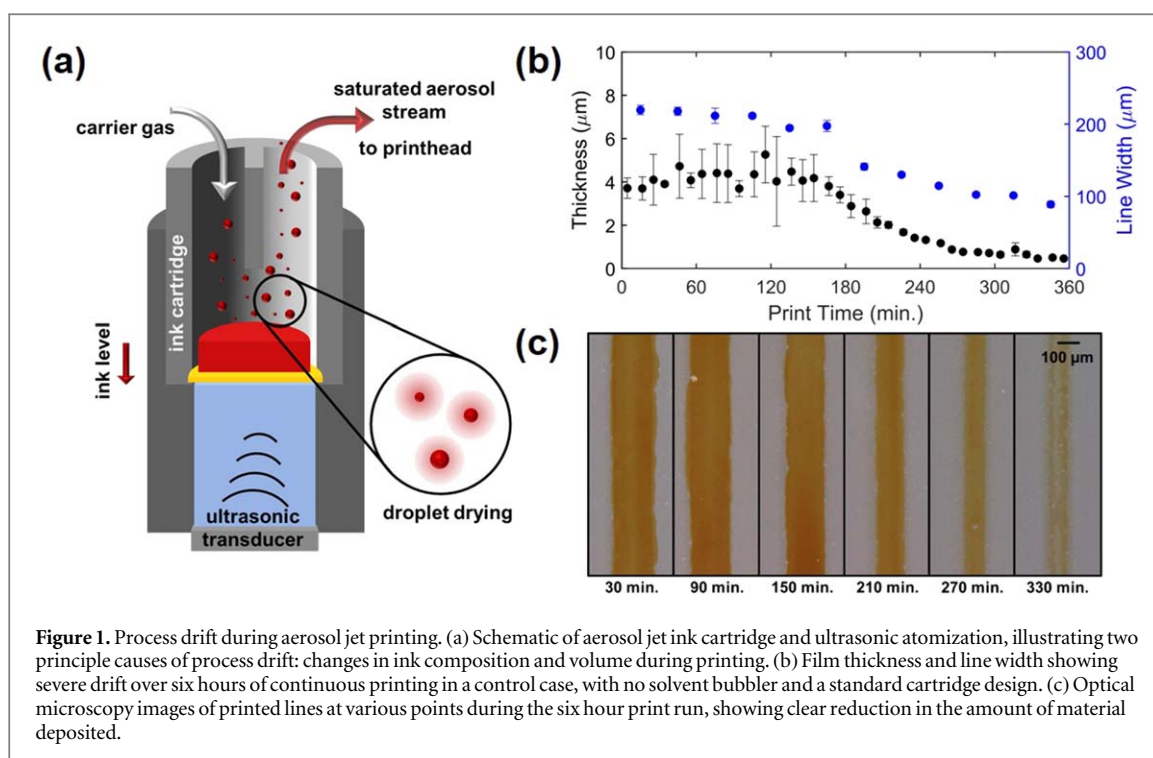
Film thickness measurements were collected using a Bruker Dektak XT stylus profilometer with 3.0 mg force and a scan speed of 0.5 mm s $^{-1}$. Profile data were analyzed using a Matlab script, with three measurements performed across each film. Line width measurements were collected using a Keyence VHX-7000 digital microscope. Automated routines were used to distinguish the line from the substrate and reduce user subjectivity in line width measurements.

Modeling

All mathematical models were implemented using Matlab software. Descriptions can be found in the supporting information, available online at stacks.iop.org/FPE/5/015009/mmedia.

Results and discussion

Experiments for this study used a custom-built printer based loosely on the IDS Nanojet architecture and described in prior work [27, 28]. This printer uses an ultrasonic atomizer and a compact cartridge, shown in figure 1(a), located immediately adjacent to the deposition nozzle (figure S1). This reduces the aerosol transport distance, limiting the settling of droplets en route to the printhead. A standard printing run was performed as a control experiment to assess the effects of process drift, as described in the Experimental Methods. A magnetite nanoparticle ink was used for these experiments, formulated for aerosol jet printing from a commercial paste, because it provides a moderately complex model system with a dual-component solvent system, dispersed nanoparticles, and an adhesion promoter [13]. This complexity provides a challenge for process drift, as any change in ink composition can alter atomization and printing characteristics, while the active component of magnetite nanoparticles is relevant for applications in security printing, power devices, sensing, and communications [29, 30]. While factors external to the printhead, such as substrate surface energy, substrate roughness, ambient temperature, and ambient humidity, are likely to have some effect on print quality, this study focuses on internal factors related to the ink and cartridge, as these are expected to dominate drift in deposition rate. Furthermore, the colloidal stability of the ink was confirmed by a series of dynamic light scattering measurements (figure S2), such that observed variations do not result from the specific ink chemistry and are expected to be generally applicable. Following printing and drying, the thickness of each film is measured by stylus profilometry and correlated to the print time. This allows straightforward analysis of drift in the deposition rate. While variation in the



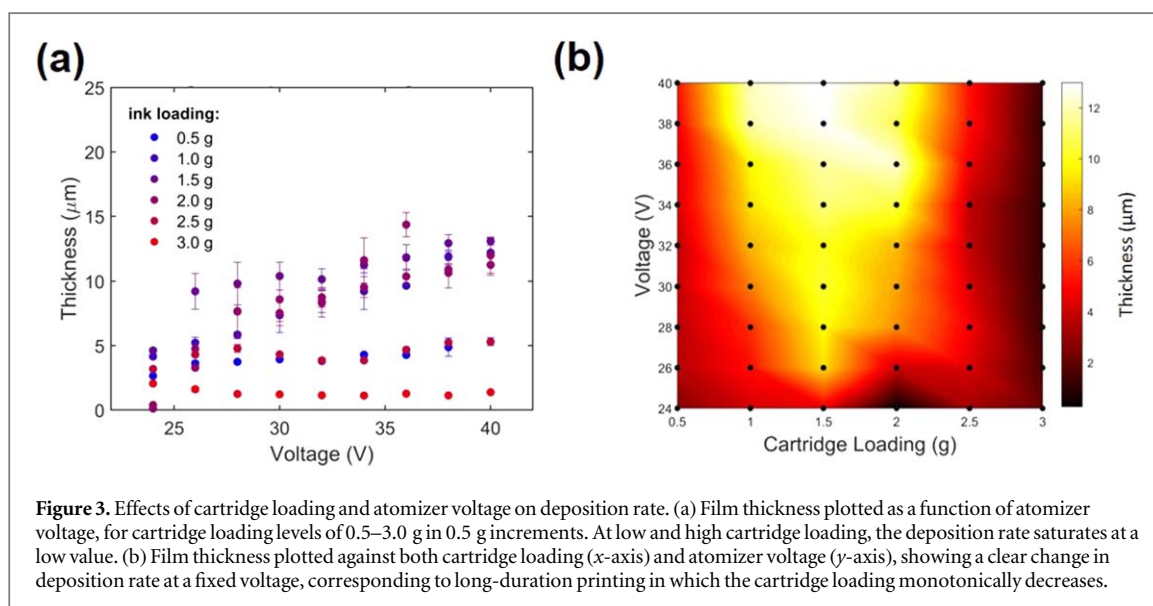
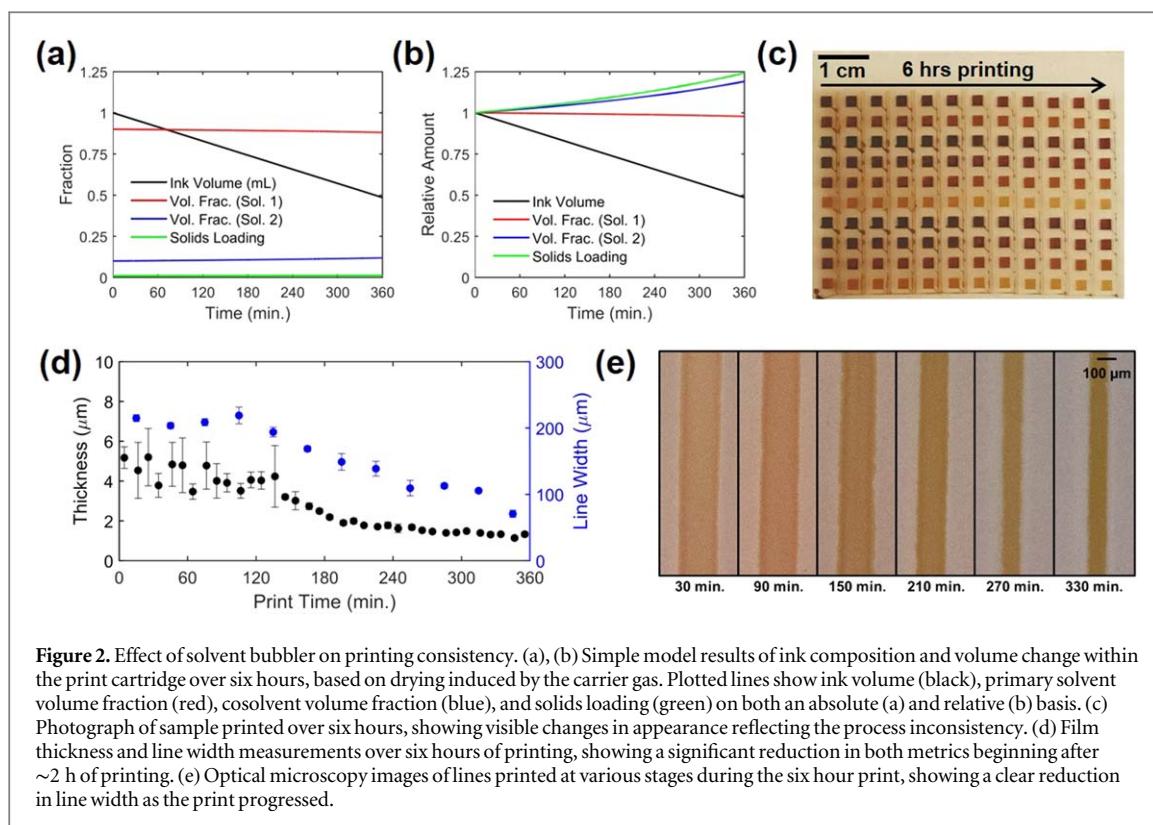
resolution is tracked, it is given lower priority, as the resolution is principally related to gas flow rates and nozzle dimensions which are fixed. Variation in the deposition rate will have indirect effects on resolution, however, so stability in this metric is critical to the process overall and representative of process drift.

The results for this baseline test are shown in figures 1(b), (c) and S3. Over the first 150 min of printing, the deposition is fairly consistent, including both the deposition rate (as measured by film thickness) and the line width. However, after this initial stable period, the deposition rate falls off dramatically, ultimately reaching a level of $12.5\% \pm 1.0\%$ of the initial value following six hours. The line width shows a similar change resulting from the reduction in deposition rate, decreasing from $219 \pm 6 \mu\text{m}$ in the first hour to $95 \pm 7 \mu\text{m}$ in the sixth. Both of these effects are consistent with a reduction in the atomization rate of the ink, and thus a lower aerosol density. Similar behavior is typical for aerosol jet printing, and presents an impediment to broader applications of the technology.

The first cause of drift we explore is well known, and is related to variation in the ink composition. During the baseline test, a dry gas is continuously flowing through the ink cartridge. Micron-scale droplets feature evaporation timescales on the order of milliseconds, and so solvent is continuously removed from the cartridge [31, 32]. This is illustrated using simple models, shown in figures 2(a), (b) and discussed in the supporting information. The case considered here is representative of the model ink, and most inks for aerosol jet printing, in that it considers a two-component ink solvent system based on a primary,

moderate volatility solvent and a secondary, less volatile solvent at 5%–20% [13, 33]. Due to the rapid nature of evaporation from micron-scale droplets, both solvents are expected to saturate the carrier gas. The low-volatility solvent typically has a much lower saturation vapor pressure, causing this component to be enhanced relative to the primary solvent. This can affect downstream drying effects induced by the sheath gas, potentially increasing the apparent deposition rate. In addition to this change in solvent composition, the solids loading of the ink increases in the cartridge. For inks near the threshold of atomization, a small resulting increase in viscosity can reduce atomization yield, thereby reducing deposition onto the substrate. This illustrates how process drift can lead to unexpected outcomes, with both an increase and decrease in deposition rate possible. As this cause of drift is well known, a partial solution is also widely adopted, namely running the carrier gas through a solvent bubbler upstream of the printhead.

When this strategy is implemented, overall printing stability is improved, as shown in figures 2(c)–(e) and S4. Figure 2(c) shows a photograph of a test sample layout for a six hour print test; drift during printing, as judged by optical appearance, can be discerned by eye. This observed difference is corroborated by film thickness and line width measurements, shown in figure 2(d). Similar to the previous case without a solvent bubbler, the ink initially prints with reasonable stability for ~ 150 min. Following this period, a decrease in deposition rate is again observed, with the final film thickness after six hours reduced to $25.5\% \pm 2.9\%$ of the initial value. As shown in figure 2(e), the line width also reflects this reduction in



aerosol density, with a decrease from $209 \pm 7 \mu\text{m}$ in the first hour to $88 \pm 19 \mu\text{m}$ in the sixth. This suggests that, while ink composition drift can have an impact, it is not the sole basis for process inconsistency. Based on the model, even if the solvent bubbler perfectly compensates for ink drying, the very process of printing changes another parameter that can affect stability, namely the volume of ink in the cartridge.

To assess the impact of the ink volume on printing, a careful study was performed in which the ink loading level was deliberately manipulated to study its effect independent of composition variations. At each ink loading level, a sweep of atomizer voltage was

performed to determine the impacts of both parameters on atomization yield. The results are shown in figure 3. At low ink loading levels ($<1.0 \text{ g}$), the deposition rate, here measured by the film thickness, saturates at fairly low values. In this regime, the deposition rate is relatively insensitive to variations in voltage, but the overall film thickness remains low. With a moderate ink loading (1.0–2.0 g), the film thickness increases steadily with increasing atomizer power. However, when the ink loading exceeds this range ($>2.0 \text{ g}$), the film thickness again shows saturation at low values. This suggests that the atomization yield is directly related to the ink volume in the cartridge. Moreover, when

the ink volume is outside of the target range, increasing the atomization power has almost no impact on atomization yield (figure S5). The primary cause of this is likely the location of the liquid surface relative to the ultrasonic atomizer. Ultrasonic nebulizers are expected to display this behavior, as the ultrasonic waves are focused on the liquid surface for maximum coupling [34, 35]. In many cases, this effect of the ink level can dominate any effects of atomizer power, and modulating the atomizer power cannot compensate for reduction in deposition rate due to ink level changes. This has important implications for extended duration printing because the liquid level is not consistent over the duration of the print. Therefore, even if the ink composition is maintained, ink utilized for printing or lost due to settling in the mist tube will affect the atomization characteristics. This is illustrated in figure 3(b), which plots the measured thickness against both cartridge loading and voltage. For a long-duration print, the voltage remains consistent, but the cartridge loading is gradually reduced. As the plot is traversed from right to left, the deposition rate initially increases to its maximum value, and then decreases, with a limited plateau. This explains the results in figure 2(d). With an initial ink loading of ~ 1.9 g, the atomization is initially near its peak efficacy. As printing progresses, the state of the cartridge moves leftward in figure 3(b), and the deposition rate drops off rather significantly after ~ 2 h print time. This behavior illustrates the challenge faced in achieving stable and consistent aerosol jet printing, and suggests that, depending on where printing starts, either an increase or decrease in atomization is expected not as an isolated problem based on the particular ink, but as an endemic feature of the atomization method itself. Moreover, a change in atomization yield will have downstream effects, including a direct impact on deposition rate and indirect impacts on line resolution and morphology. Because this behavior is linked to the atomization mechanism, in this case ultrasonic atomization, these results are unlikely to translate directly to pneumatic atomization systems. However, the observation that cartridge loading can affect atomization in a general sense merits further investigation for pneumatic systems, and efforts here to mitigate changes in the ink level may have broader applicability.

The identification of ink level as a critical factor in atomization yield motivates strategies to control and stabilize the cartridge loading. Direct addition of ink or solvent to the cartridge has been proposed, but would need to be perfectly compensated to the ink usage, which precludes generalization in a straightforward manner given the wide variation in inks and process parameters used. Here, we develop a recirculating ink cartridge to both maintain ink level in the cartridge and buffer slow changes in ink composition with a larger reservoir, as shown in figure 4(a). In order to implement this strategy, the ink cartridge is redesigned and fabricated using stereolithography to

accommodate a continuous ink recirculation loop, as shown in figure 4(b). A miniature peristaltic pump is used to circulate the ink, isolating the pump from ink solvents. The peristaltic pump is controlled digitally using an Arduino, allowing speed and direction to be adjusted as needed.

Using this recirculating ink cartridge, an extended duration test of printing stability was performed using the magnetite nanoparticle ink. As before, large grids of 2×2 mm films were used to track the deposition rate. Optical images of the samples illustrate the reasonable degree of uniformity over 30 h of printing spanning 5 print runs (figure 4(c)). The film thickness measurements (figure 4(d)) corroborate this, showing some fluctuations but limited systematic drift over the duration of printing. While some variation is clear, particularly on the third print run, this is reset at the beginning of the following run and does not propagate. Such effects could presumably be avoided by programming stops during the print run at regular intervals to reset the cartridge condition without human intervention, providing a benefit over a more labor-intensive manual reset of the system. Overall, the film thickness increases to $131\% \pm 13\%$ of the initial value following 30 h printing, and during the last 18 h of printing the measured film thickness varies with a relative standard deviation of 17%. Analysis of the printed lines, shown in figure 4(e), is consistent with these results, with a 9.4% relative standard deviation in line width over the full 30 h (figure S6). In addition, although a solvent bubbler is employed for this work, it is not expected to fully saturate the carrier gas, and thus small changes in composition are expected. The use of an external reservoir, in this case with 10 ml ink initially loaded, will buffer these changes over a larger volume. At the end of 30 h of printing, the amount of ink in the reservoir was decreased to the extent that air was being drawn into the pump, thus prompting the end of the experiment. However, for applications requiring a longer print duration, simply increasing the reservoir size is straightforward and economical. Moreover, this strategy is independent of the specific ink properties, and can thus be applied to alternative materials (figures S7, S8), providing a practical and general tool to address this key challenge in aerosol jet printing.

Conclusions

Overall, this study demonstrates the influence of ink level variation on process drift during aerosol jet printing and proposes a simple and general strategy to mitigate drift. This allows extended print duration, here up to 30 h, with little observed systematic drift. While this does not address short-term variability, it provides opportunities to more confidently optimize and study the process without the persistent challenges of instability. In addition, this method addresses the

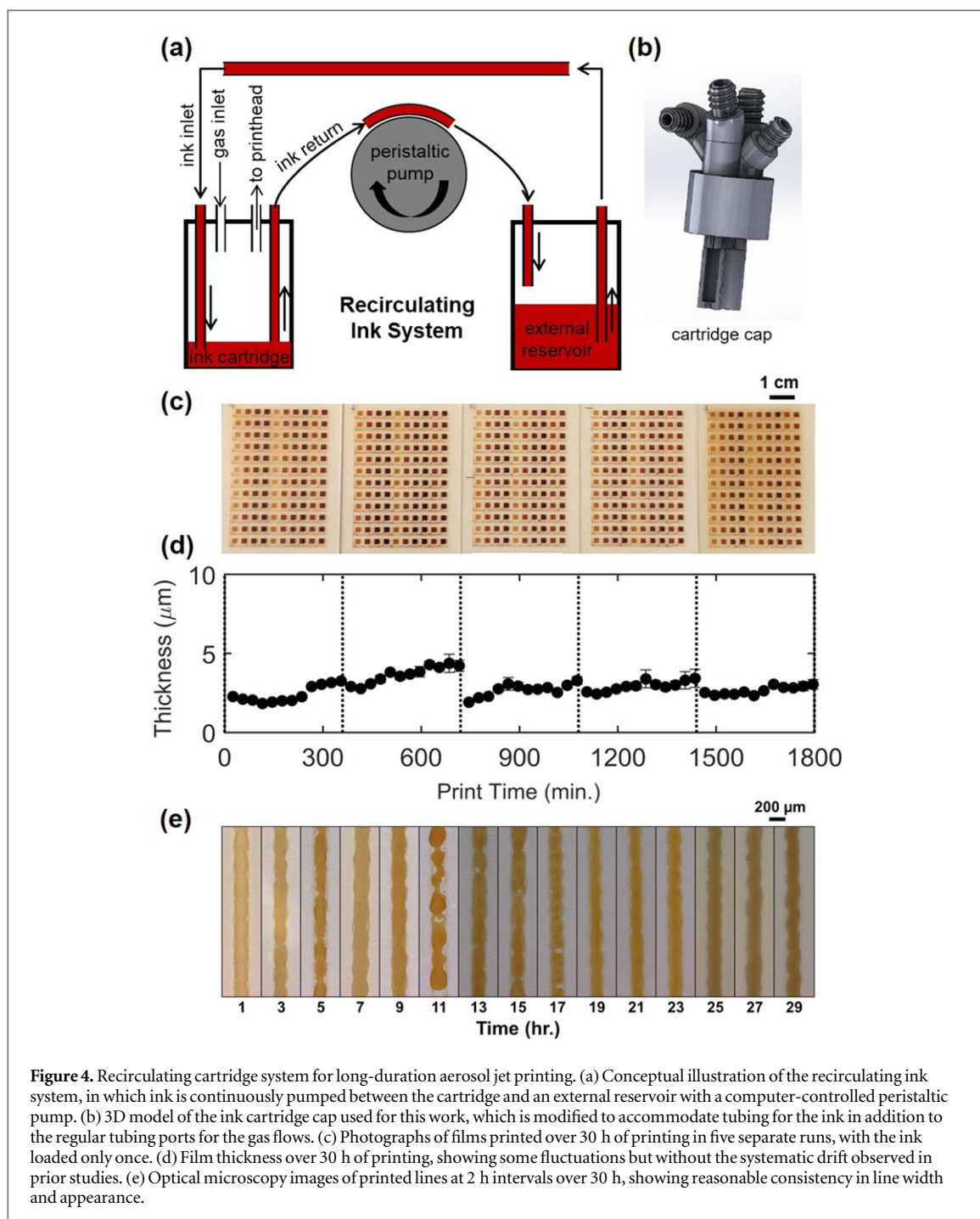


Figure 4. Recirculating cartridge system for long-duration aerosol jet printing. (a) Conceptual illustration of the recirculating ink system, in which ink is continuously pumped between the cartridge and an external reservoir with a computer-controlled peristaltic pump. (b) 3D model of the ink cartridge cap used for this work, which is modified to accommodate tubing for the ink in addition to the regular tubing ports for the gas flows. (c) Photographs of films printed over 30 h of printing in five separate runs, with the ink loaded only once. (d) Film thickness over 30 h of printing, showing some fluctuations but without the systematic drift observed in prior studies. (e) Optical microscopy images of printed lines at 2 h intervals over 30 h, showing reasonable consistency in line width and appearance.

core causes of drift and could be readily combined with higher level monitoring and feedback strategies. By decoupling the ink volume in the cartridge from an external reservoir, small composition changes can be buffered. Moreover, this provides opportunities for monitoring the ink, rather than the aerosol stream, by improving access external to the cartridge, thus establishing a framework to address true causes of drift rather than symptoms.

Acknowledgments

This work was generously supported by the Harry S Truman Fellowship through the Laboratory Directed

Research and Development program at Sandia National Laboratories. Sandia National Laboratories is a multi-program laboratory managed and operated by National Technology and Engineering Solutions of Sandia, LLC, a wholly owned subsidiary of Honeywell International, Inc., for the US Department of Energy's National Nuclear Security Administration under contract DE-NA-0003525. The authors would also like to thank Adam W Cook, Bryan J Kaehr, and P Randall Schunk of Sandia National Laboratories for helpful discussions and access to laboratory facilities to support this work. This paper describes objective technical results and analysis. Any subjective views or opinions that might be expressed in the paper do not

necessarily represent the views of the US Department of Energy or the United States Government.

Notes

The authors declare no competing financial interest.

ORCID iDs

Ethan B Secor  <https://orcid.org/0000-0003-2324-1686>

References

- [1] Fukuda K and Someya T 2017 *Adv. Mater.* **29** 1602736
- [2] Lupo D, Clemens W, Breitung S and Hecker K 2013 *Applications of Organic and Printed Electronics* ed E Cantatore (New York: Springer) pp 1
- [3] Nathan A *et al* 2012 *Proc. IEEE* **100** 1486
- [4] Hoey J M, Lutfurakhmanov A, Schulz D L and Akhatov I S 2012 *J. Nanotechnol.* **2012** 324380
- [5] Sarobol P, Cook A, Clem P G, Keicher D, Hirschfeld D, Hall A C and Bell N S 2016 *Annu. Rev. Mater. Res.* **46** 41
- [6] Wilkinson N J, Smith M A A, Kay R W and Harris R A 2019 *Int. J. Adv. Manuf. Tech.* **105** 4599
- [7] Christenson K K, Paulsen J A, Renn M J, McDonald K and Bourassa J 2011 Digital printing of circuit boards using aerosol jet *Int. Conf. on Digital Printing Technologies* (Society for Imaging Science and Technology) p 433
- [8] Gupta A A, Bolduc A, Cloutier S G and Izquierdo R 2016 Aerosol jet printing for printed electronics rapid prototyping 2016 *IEEE ISCAS (Montreal, QC, Canada)* (Piscataway, NJ: IEEE) pp 866
- [9] Saleh M S, Hu C and Panat R 2017 *Sci. Adv.* **3** e1601986
- [10] Seifert T, Baum M, Roscher F, Wiemer M and Gessner T 2015 *Mater. Today-Proc.* **2** 4262
- [11] Cao C, Andrews J B and Franklin A D 2017 *Adv. Electron. Mater.* **3** 1700057
- [12] Ha M, Xia Y, Green A A, Zhang W, Renn M J, Kim C H, Hersam M C and Frisbie C D 2010 *ACS Nano* **4** 4388
- [13] Hong K, Kim Y H, Kim S H, Xie W, Xu W D, Kim C H and Frisbie C D 2014 *Adv. Mater.* **26** 7032
- [14] Bag S, Deneault J R and Durstock M F 2017 *Adv. Energy Mater.* **7** 1701151
- [15] Mette A, Richter P L, Hörteis M and Glunz S W 2007 *Prog. Photovolt., Res. Appl.* **15** 621
- [16] Williams B A, Mahajan A, Smeaton M A, Holgate C S, Aydil E S and Francis L F 2015 *ACS Appl. Mater. Interfaces* **7** 11526
- [17] Agarwala S, Goh G L, Dinh Le T S, An J, Peh Z K, Yeong W Y and Kim Y J 2019 *ACS Sens.* **4** 218
- [18] Eckstein R, Rödlmeier T, Glaser T, Valouch S, Mauer R, Lemmer U and Hernandez-Sosa G 2015 *Adv. Electron. Mater.* **1** 1500101
- [19] Goh G L, Agarwala S, Tan Y J and Yeong W Y 2018 *Sensors Actuators B* **260** 227
- [20] Zhao D, Liu T, Zhang M, Liang R and Wang B 2012 *Smart Mater. Struct.* **21** 115008
- [21] Smith M, Choi Y S, Boughey C and Kar-Narayan S 2017 *Flex. Print. Electron.* **2** 015004
- [22] Gu Y, Gutierrez D, Das S and Hines D R 2017 *J. Micromech. Microeng.* **27** 097001
- [23] Salary R, Lombardi J P, Rao P K and Poliks M D 2017 *J. Manuf. Sci. Eng.* **139** 101010
- [24] Salary R, Lombardi J P, Samie Tootooni M, Donovan R, Rao P K, Borgesen P and Poliks M D 2017 *J. Manuf. Sci. Eng.* **139** 021015
- [25] Binder S, Glatthaar M and Rädlein E 2014 *Aerosol Sci. Technol.* **48** 924
- [26] Chen G, Gu Y, Tsang H, Hines D R and Das S 2018 *Adv. Eng. Mater.* **20** 1701084
- [27] Secor E B 2018 *Flex. Print. Electron.* **3** 035002
- [28] Secor E B 2018 *Flex. Print. Electron.* **3** 035007
- [29] Kolchanov D S, Slabov V, Keller K, Sergeeva E, Zhukov M V, Drozdov A S and Vinogradov A V 2019 *J. Mater. Chem. C* **7** 6426
- [30] Leigh S J, Purssell C P, Billson D R and Hutchins D A 2014 *Smart Mater. Struct.* **23** 095039
- [31] Widmann J F and Davis E J 1997 *Aerosol Sci. Technol.* **27** 243
- [32] Williams B A, Trejo N D, Wu A, Holgate C S, Francis L F and Aydil E S 2017 *ACS Appl. Mater. Interfaces* **9** 18865
- [33] Mahajan A, Frisbie C D and Francis L F 2013 *ACS Appl. Mater. Interfaces* **5** 4856
- [34] Al-Jumaily A M and Meshkinzar A 2017 *Adv. Acoust. Vib.* **2017** 7861726
- [35] Simon J C, Sapozhnikov O A, Khokhlova V A, Crum L A and Bailey M R 2015 *J. Fluid Mech.* **766** 129